Triad Resonance as a Mechanism for Internal Wave Dissipation

Lisa Neef

University of Toronto

1 Introduction

Breaking of internal waves, i.e. the nonlinear transfer of energy from internal waves to turbulence, drives deep ocean mixing. Both the sources and sinks of internal wave energy in the world ocean, however, are spatially variable. It is estimated that roughly half of internal wave energy in the ocean is produced by the movement of the barotropic tide around topography, which generates internal waves with the same frequency. Where and when mixing due to the internal tide occurs, depends on two factors: the strength of the internal tide generated around a particular piece of topography, and the mechanisms that cause this internal tide to cascade into smaller scales, which then break and cause mixing. The magnitude and distribution in time and space of neither of these is well understood.

Much research is currently focused on how efficiently a particular topographic structure generates an internal tide. Furthermore, it is not well understood how far, in each case, a particular internal tide will propagate, and where and by what mechanisms it will deposit its energy. Recent studies(e.g. [1], [2]) have suggested that mixing due to internal wave breaking happens to a large extent in "hotspots" near rough topography.

MacKinnon and Winters [3] showed, using an idealized model, that an internal tide of M_2 frequency seems to efficiently break into waves of roughly half the M_2 frequency, and smaller vertical scale, suggesting that Parametric Subharmonic Instability (or PSI, i.e. the class of resonant wave-wave interactions wherein energy is transferred from a primary wave to two recipient waves of half the primary frequency and smaller vertical scale, and the range of interactions where the secondary waves are near this half-frequency) could be a significant mechanism of energy transfer to smaller scales. The efficiency of this interaction increased dramatically as the waves approached the critical latitude where the $M_2/2$ frequency equals the inertial frequency (f). The results of MacKinnon and Winters suggest not only that PSI could be a significant mechanism of energy transfer out of the internal M_2 tide, but also that this mechanism is strongly latitude-dependent. Though PSI has previously been thought too slow ([4]) to be an important mechanism for the transfer of energy into smaller-scales, MacKinnon and Winters argue that it might be much faster than previously thought in the nearfield of the generation site, where the internal tide is coherent.

In regards to latitude dependence, it is not clear why the efficiency of these interactions should increase so much near the critical latitude. One factor could be the fact that, near

the critical latitude, the waves with frequencies close to the subharmonic frequency have group velocities near zero, and, by breaking close to where they are generated, could create a "hotspot", where mixing is several times stronger than at lower latitudes. It is not yet known, however, how the efficiency of PSI interactions themselves actually changes with latitude, regardless of the group velocity of the resulting subharmonic waves. If PSI is indeed a significant factor in internal wave breakingg, its latitude dependence must be carefully examined.

The purpose of this paper is to find the intrinsic dependence of PSI interactions on latitude, or, more precisely, on the inertial frequency, f.

This will be done by rederiving the well-known triad equations for the case of internal waves with rotation of the earth (Section 2), and then integrating them numerically (Section 3). Section 4 then compares the results of the numerical integration to the established analytical solutions to the problem.

The greater purpose of this study is to help improve understanding of the spatial and temporal structure of tidal mixing, that is, how and where energy is transferred out of the internal tide. This is necessary in order to better understand the structure of the global ocean circulation, which requires both a map of the tidal generation sites, as well as a dynamical understanding of how much energy from the internal tide is lost to dissipation. Before PSI is dismissed as a dissipation mechanism, it must be considered for a coherent primary wave, and its latitude dependence examined. Understanding of this dependence is necessary for the correct modeling of energy dissipation of the internal tide.

2 Resonant Triad Model of Weakly Nonlinear Interactions

2.1 Derivation

We begin with the governing equations,

$$\frac{\partial u}{\partial t} + \mathbf{u} \cdot \nabla u - fv = -\frac{1}{\rho_0} \frac{\partial p}{\partial x} \tag{1}$$

$$\frac{\partial v}{\partial t} + \mathbf{u} \cdot \nabla v + fu = -\frac{1}{\rho_0} \frac{\partial p}{\partial y} \tag{2}$$

$$\frac{\partial w}{\partial t} + \mathbf{u} \cdot \nabla w = -\frac{1}{\rho_0} \frac{\partial p}{\partial z} - \rho' g \tag{3}$$

$$\frac{\partial \rho'}{\partial t} + w \frac{d\rho_0}{dz} = 0 \tag{4}$$

$$\nabla \cdot \mathbf{u} = 0. \tag{5}$$

One possible way to approximate weakly nonlinear interactions is via a resonant triad model. It is helpful to nondimensionalize by characteristic length, velocity, and time scales, so that different scales of motion can be examined. We thus scale the variables by typical velocity u_*, length scale k_*, and the time scale ω_*^{-1} of our primary wave, a typical propagating

internal tide. Thus,

$$(u, v, w)^{\mathrm{T}} = u_*(\tilde{u}, \tilde{v}, \tilde{w})^{\mathrm{T}} \tag{6}$$

$$x = \frac{\tilde{x}}{k_*} \tag{7}$$

$$t = \frac{\tilde{t}}{\omega_*} \tag{8}$$

where tildes indicate nondimensional quantities. The pressure-gradient terms on the right hand side must have the same dimensions as the left hand side. If we assume that the linear terms are dominant, the pressure-gradient terms must scale like the linear terms on the left hand side:

$$p = \frac{\rho_0 u_*}{k_* t_*} \tilde{p}. \tag{9}$$

We also define a nondimensional inertial and buoyancy frequencies, respectively,

$$f = \tilde{f}\omega_*, \tag{10}$$

$$N = \tilde{N}\omega_* \tag{11}$$

which are both scaled with respect to the linear wave motion.

Plugging (6) - (9) into (1) - (5), we have

$$\frac{d\tilde{u}}{d\tilde{t}} = -\frac{1}{\rho_0}\frac{d\tilde{p}}{d\tilde{x}} - \frac{u_* k_*}{\omega_*}\tilde{\mathbf{u}} \cdot \nabla\tilde{u} + \tilde{f}\tilde{v}, \tag{12}$$

and similar equations for $\tilde{v}$ and $\tilde{w}$. The nonlinear terms in these equations will be small if the quantity

$$\epsilon := \frac{u_*}{\omega_*/k_*} \tag{13}$$

is small. (13) shows that ϵ is the ratio of typical particle speed to the typical phase speed of the waves.

Equations (1)-(5) can be combined into a single equation:

$$\partial_{tt}(-\nabla^2 - \partial_{zz})w - N^2\nabla^2 w - f^2\partial_{zz}w$$
$$-\epsilon[\nabla^2(\mathbf{u} \cdot \nabla b) - \partial_t\nabla^2(\mathbf{u} \cdot \nabla w) + \partial_{xzt}(\mathbf{u} \cdot \nabla u) + \partial_{yzt}(\mathbf{u} \cdot \nabla v) -$$
$$f\partial_{yz}(\mathbf{u} \cdot \nabla u) + f\partial_{xz}(\mathbf{u} \cdot \nabla u)] = 0 \tag{14}$$

A useful tool for describing the impact of weakly nonlinear interactions on the linear dynamics is to define multiple time scales of motion. Having already defined a typical time scale of the primary wave, and nondimensionalized the governing equations by this time scale, we now introduce a comparatively *slow* timescale,

$$\tau = \epsilon t_* \tilde{t}, \tag{15}$$

with corresponding nondimensional time

$$\tilde{\tau} = \epsilon\tilde{t}. \tag{16}$$

166

$\tilde{\tau}$ is defined with respect to the magnitude of the nonlinear terms.

The time derivatives in (14) then become

$$\frac{\partial}{\partial t} \quad \rightarrow \quad \frac{\partial}{\partial t} + \epsilon \frac{\partial}{\partial \tau} \tag{17}$$

$$\frac{\partial^2}{\partial t^2} \quad \rightarrow \quad \frac{\partial^2}{\partial t^2} + 2\epsilon \frac{\partial^2}{\partial t \partial \tau} + \epsilon^2 \frac{\partial^2}{\partial \tau^2} \tag{18}$$

Substituting the right hand sides of (17) and (18) into (14), the $\mathcal{O}(\epsilon^0)$ balance is

$$\partial_{tt}(-\nabla^2 - \partial_{zz})w - N^2\nabla^2 w - f^2\partial_{zz}w = 0. \tag{19}$$

This is the linear component, and admits wave solutions like

$$w = w_i e^{i(k_i x + l_i y + m_i z - \omega_i t)} = \Sigma w_i e^{i\theta_i}, \tag{20}$$

with ω_i subject to the dispersion relation

$$\omega_i^2 = \frac{N^2\left(k_i^2 + l_i^2\right) + f^2 m_i^2}{k_i^2 + l_i^2 + m_i^2} \tag{21}$$

Substituting the linear solution (20) into the linear parts of (1) - (5), we can find polarization relations which relate u, v, p, and b to the prognostic variable, w:

$$u = g_u(w) = \left(\frac{m(ik\omega - fl)}{i\omega(k^2 - l^2)}\right)w \tag{22}$$

$$v = g_v(w) = \left(\frac{m(ik\omega - fk)}{i\omega(k^2 - l^2)}\right)w \tag{23}$$

$$p = g_p(w) = \left(\frac{\omega^2 - N^2}{m\omega}\right)w \tag{24}$$

$$b = g_b(w) = \frac{-iN^2}{\omega}w \tag{25}$$

The $\mathcal{O}(\epsilon)$ balance is

$$2\frac{\partial^2}{\partial t \partial \tau}(\nabla^2 + \partial_{zz})w =$$

$$-\nabla^2(\mathbf{u} \cdot \nabla b) - \partial_t\nabla^2(\mathbf{u} \cdot \nabla w) + \partial_{zxt}(\mathbf{u} \cdot \nabla u) + \partial_{zyt}(\mathbf{u} \cdot \nabla v) - f\partial_{zy}(\mathbf{u} \cdot \nabla u) + f\partial_{zx}(\mathbf{u} \cdot \nabla v), \tag{26}$$

where ∇^2 is the horizontal Laplacian.

In order to model the nonlinear interaction as described by (26), we will seek solutions like

$$w = \sum z(\tau)e^{i(k_i x + l_i y + m_i z - \omega_i t)} + \sum z_i^*(\tau)e^{-i(k_i x + l_i y + m_i z - \omega_i t)} = \sum z_i(\tau)_i e^{i\theta_i} + c.c. \tag{27}$$

(27) is a sum of solutions to the linear problem. The complex amplitudes $z_i(\tau) = w_i(\tau)e^{i\phi_i}$ are allowed to vary on the slow timescale, to reflect the nonlinear interactions between the component waves.

(27) can then be substituted into (26) . Individual terms on the right hand side will then look like

$$
\begin{aligned}
\mathbf{u} \cdot \nabla s &= u_1(\frac{\partial s_2}{\partial x} + \frac{\partial s_3}{\partial x} + ...) + u_2(\frac{\partial s_1}{\partial x} + \frac{\partial s_3}{\partial x} + ...) + v_1(\frac{\partial s_2}{\partial y} + \frac{\partial s_3}{\partial y} + ...) + ... \\
&= u_1 (k_2 s_2 + k_3 s_3 + ...) + u_2 (k_1 s_1 + k_3 s_3 + ...) + v_1 (l_2 s_2 + l_3 s_3 + ...) + ... \\
&= \sum_i u_i \sum_{j \neq i} k_j s_j + \sum_i v_i \sum_{j \neq i} l_j s_j + \sum_i w_i \sum_{j \neq i} m_j s_j
\end{aligned}
\tag{28}
$$

where s is can be one of the four system variables u, v, w, b.

Using the polarization relations (22)-(25), individual terms in (28) can be written in terms of the amplitudes z_i and phases θ_i of each component wave, e.g.

$$
u_i k_j s_j = z_i g_u (z_i) e^{i\theta_i} k_j g_s (z_j) z_j e^{i\theta_j}.
\tag{29}
$$

Consequently, derivatives of terms like $\mathbf{u} \cdot \nabla s$ will bring down factors of $k_i + k_j$, $l_i + l_j$, $m_i + m_j$, and $\omega_i + \omega_j$.

Plugging (27) into the left hand side of (26) gives

$$
2i \sum_k \omega_k \left(k_k^2 + l_k^2 + m_k^2 \right) \frac{\partial z_k}{\partial \tau} e^{i\theta_k}.
\tag{30}
$$

If we now consider the evolution of a particular wavenumber component (k_0, m_0, ω_0) by averaging both the left hand side and the right hand side over the period of that wave, the terms on the right hand side that will balance the left hand side will be ones where

$$
\theta_i + \theta_j = \theta_0.
\tag{31}
$$

The simplest possible nonlinear interaction we can consider is therefore a triad of waves where (31) holds, or, more specifically, where

$$
\begin{aligned}
k_1 + k_2 &= k_0 \tag{32} \\
l_1 + l_2 &= l_0 \tag{33} \\
m_1 + m_2 &= m_0 \tag{34} \\
\omega_1 + \omega_2 &= \omega_0. \tag{35}
\end{aligned}
$$

The equations for this interaction found by truncating (26) for the triad of waves, so that (27) becomes

$$
w = \sum_{i=1}^{3} z_i(\tau) e^{i\theta_i(t)} + c.c. = \sum_{i=1}^{3} w_i(\tau) e^{i(\theta_i(t) + \phi_i(\tau))} + c.c.
\tag{36}
$$

Plugging (36) into (26) and factoring out the complex exponentials in the individual terms as in (29) and (30), and applying the resonance condition (31), such that the phases of the individual waves, $e^{i\theta_i}$ divide out, we are left with equations for the evolution of the

complex wave amplitudes, $z_i(\tau)$, on the "slow" time scale (see Appendix for details). The resulting model is then given by

$$\dot{z}_0 = -i\Gamma_0 z_1 z_2 \tag{37}$$

$$\dot{z}_1 = -i\Gamma_1 z_0 z_2^* \tag{38}$$

$$\dot{z}_2 = -i\Gamma_2 z_0 z_1^* \tag{39}$$

where the ∂_τ time derivative has been replaced with a dot. For each wave, the corresponding interaction coefficient Γ_i is a function of the wavenumbers of the two interacting waves. The interaction coefficients are derived in the appendix.

2.2 Comments

1. It is important to remember that the system (37) - (39) describes the coupled fluctuations of the amplitudes of the three waves, not the waves themselves. However, the individual fields of each variable can be found, for each wave, by substituting the amplitudes w_i of each wave, and the appropriate wave numbers, into the polarization relations (22) - (25). The frequency of the actual waves will be proportional to that of the triad interaction by a factor of ϵ.

2. The appropriate combinations of wavenumbers cannot be arbitrary, but must be chosen so that both the dispersion relation (21) and the resonance condition for each dimension (32) - (35) are satisfied. Thus, for example, given some horizontal structure described by (fixed) horizontal wave numbers k_i and l_i, decreasing ω_i means that the corresponding set of available vertical wavenumbers m_i will have larger values.

3. While the triad equations (37) - (39) can be easily integrated numerically, it is trickier to find resonant sets of wavenumbers and frequencies which also satisfy the dispersion relation. For example, suppose that the frequency, ω_0 and spatial wavenumbers k_0, l_0, m_0 of the primary wave are known. This leaves eight unknown parameters, but the system is then constrained by four resonance equations (32) - (35) and two dispersion relations, leaving two degrees of freedom. Thus, given the primary wave, it is only possible to choose two more wavenumbers in either one of the two secondary waves, say, for example, k_1 and l_1. In this case, k_2 and l_2 will be given by the appropriate resonance conditions, and m_1, m_2, ω_1, and ω_2 must be found by solving the system of equations given by the remaining resonance conditions (34), (35), and the dispersion relations (21) for wave 1 and wave 2. Such a system is impossible to solve analytically, but can be solved numerically.

4. It is easily seen from the triad equations (37) - (39) that the amplitude of energy exchange for each wave is proportional to the interaction coefficient for that wave – the wave with the smallest interaction coefficient exchanges the least amount of energy. It is also clear from the triad equations that the amplitude of energy exchange also depends on the initial amplitudes of the waves themselves, and their phases relative to each other.

169

5. The rate of change of each wave amplitude, and therefore the triad interaction frequency, is also a function of the initial amplitudes, and the interaction coefficients. It is this interaction frequency, and its dependence on the three sets of wavenumbers, on which this study focuses. It will be computed numerically in section 3, and analytically in section 4.

2.3 Methodology

In this study, we are interested in systems where the secondary waves (waves 1 and 2) have horizontal structures similar to that of the primary wave (wave 0), frequencies that are fractions of the primary wave frequency, and the appropriate vertical structures that result from satisfying both the dispersion relation (21) and the resonance conditions (32) - (35) . We therefore fix the parameters of the primary wave, with $\omega_0 = 1$ and k_0, l_0, and m_0 equal to three values given in Table 1. In order to simplify the problem, we choose $l_0 = l_1 = l_2 = 0$, thus reducing the problem to two dimensions while preserving the presence of the planet's rotation. This leaves one degree of freedom, which we choose to be ω_1. Now, varying ω_1, the corresponding ω_2, k_1, and k_2, m_1, and m_2 can be computed from the problem's constraints. We are thus in effect varying the frequency of the secondary waves and computing the corresponding horizontal and vertical structures.

For a given ω_1, there exists a set of possible combinations of m_1 and k_1, with consequent parameters for wave 2 given by the resonance condition. This is shown graphically in Figure 1, a plot of the vertical wavenumbers m_1 that satisfy each choice of ω_1. This so-called resonant trace has four different branches, two of which have large vertical wavenumbers as $\omega_{1,2} \to \omega_0$. The interaction coefficients in (37)-(39), and thus the interaction frequency, will be different for each branch.

The interaction frequency along these resonance traces will also depend on the other parameters in the dispersion relation, namely the buoyancy frequency, N, and the inertial frequency, f. Since the focus of this study is on the effect of latitude on the triad interaction, N will be kept constant ($N = 10$, in nondimensional units), while f will vary from 0 to $\omega_0/2$. For given $f > 0$, only those triads with $\omega_{1,2} \geq f$ will be allowed by the dispersion relation, thus truncating the resonant trace outside of the interval $[f, \omega_0 - f]$.

3 Numerical Results

Figure 2 shows the exchange of energy between three waves satisfying the resonance conditions, for a simple case where $f = 0$ and the primary wave is about an order of magnitude larger than the two daughter waves. The wavenumbers of the resonant triad in this example are given in Table 1. The corresponding fluctuation of a single wave, wave 0, is shown in Figure 3, where we have chosen $\epsilon = 0.05$. Figure 4 shows the composite wave field $w(x, z)$ for the same example, at $t = 0$ and again at a time halfway through the period of the wave interaction. At the half-period time, the vertical structure is considerably smaller, simply because Wave 2 ($m_2 = 13.36$) is dominant.

In this example, the frequency of energy exchange is about 0.75, on the nondimensional slow timescale. This means that exchange of energy between the triad members happens at a fraction of 0.75ϵ of the frequency of the primary wave, ω_0.
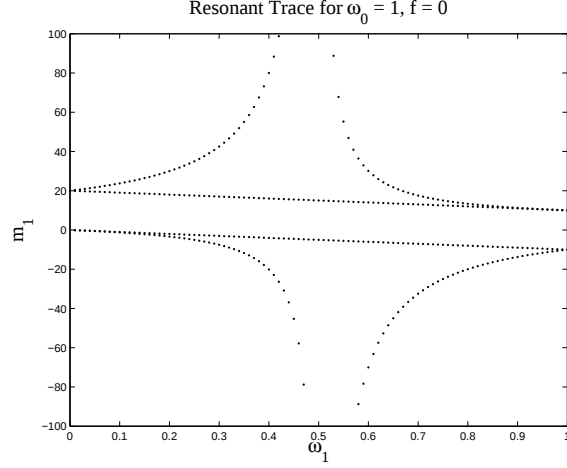
Figure 1: Pairs of frequency and vertical wavenumber satisying the resonance condition and dispersion relation, for $\omega_0 = 1$ and $l_0 = l_1 = l_2 = 0$.

Wave	Initial Amplitude w_i	Initial Phase ϕ_i	ω	k	m	Γ_i
0	1.0	3	-1	-1	10	-40.3
1	0.04	5	0.49	.12.1	-246	-4.74
2	0.02	5	0.51	-13.1	256	-5.34

Table 1: Initial values, wavenumbers, and interaction coefficients of the component waves in a sample resonant triad.
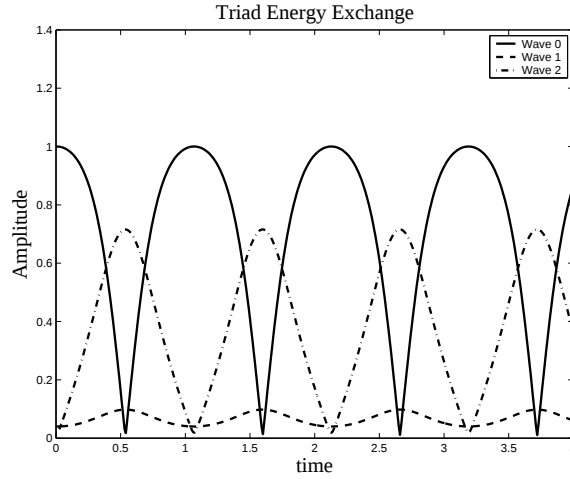
Figure 2: Exchange of energy between the three waves in a resonant triad. In this example, $f = 0$, and the wave frequencies are $\omega_0 = 1$, $\omega_1 = 0.2$, $\omega_2 = 0.8$. Initial wave amplitudes and phases are given in Table 1.

171
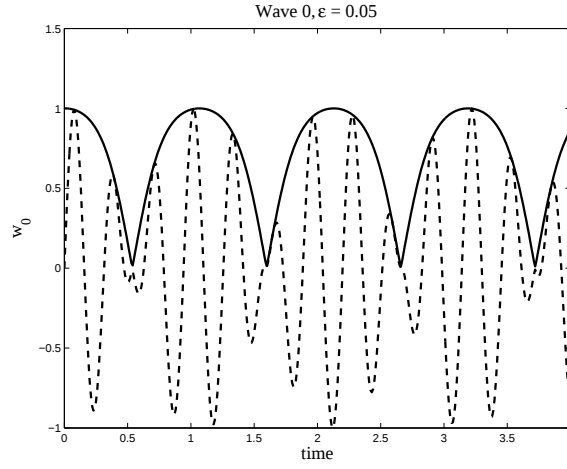
Figure 3: Amplitude fluctuation of the primary wave, for a triad oscillation with $f = 0$, and the wave frequencies and amplitudes as in Fig. 2.
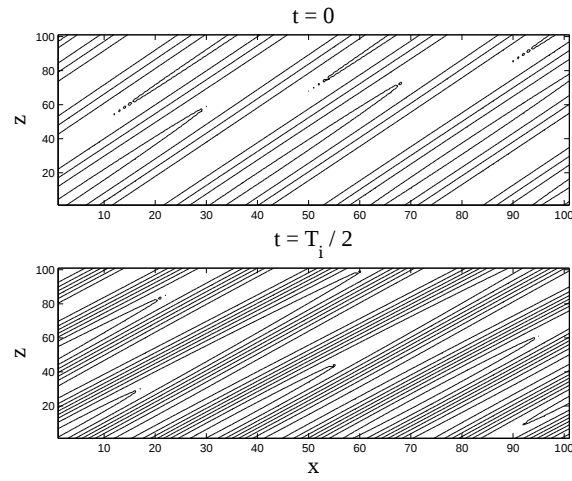

Figure 4: Fields of the variable w as a composite of the three interaction waves in the triad, at the initial time (left) and at $t = T/2$, where T is the period of the triad interaction.

172

Figure 5 examines the interaction frequency for triads with $\omega_0 = 1$, and values of ω_1 varying over the interval $[f, \omega_0/2]$ (with ω_2 changing in the other direction, to satisfy (35)). This plot has different characteristic curves, corresponding to the different branches of the resonant trace (Fig. 1). As shown in Figure 1, for a given value of ω_1, and taking $l_0 = l_1 = l_2 = 0$, there are typically three or four possible wave number combinations that satisfy both the dispersion relation and the resonance condition. Hence, a plot of the interaction frequency as a function of ω_1 has several different characteristic curves of interaction frequency. Four different increasing values of f are shown. Triads where $m_1 > 5m_0$ are indicated with an x. These indicate daughter waves with small vertical structure, the waves most likely to break and cause mixing.

For $f = 0$ the interaction frequency varies slowly with $\omega_{1,2}$, with a *minimum* at $\omega_{1,2} = \omega_0/2$. For increasing f, however, one of the resonant curves develops a sharp rise in the interaction frequency as $\omega_{1,2} \to \omega_0/2$. These are precisely those resonant triads where $m_1 > 5m_0$. As f approaches $\omega_0/2$ (the critical latitude), the band of available values of $\omega_{1,2}$ becomes smaller. This result is well known. It is surprising, however, that the overall interaction frequency seems to increase with increasing f.

Figure 6 shows the interaction frequency as a function of the three interaction coefficients, for the case $f = 0$. For each particular Γ_i, there exists usually more than one set of corresponding Γ_j, Γ_k, and thus more than one corresponding interaction frequency, making these figures difficult to interpret.. The dependence of the interaction coefficients on the resonant sets of wavenumbers (see Appendix), is similarly complicated. We now appeal to known analytical solutions to the triad equations to shed light on why the above numerical results are what they are.

4   Analytical Solution

It is possible to find an analytic solution to the system of triad equations (37) - (39), by deriving the system's invariants and transforming it into a single ODE.

First, it is helpful to transform the wave amplitudes so as to make the equations symmetric. This can be done by defining three "stretched" new wave amplitudes,

$$z_0 = \frac{\zeta_0}{2\sqrt{\Gamma_1\Gamma_2}} \tag{40}$$

$$z_1 = \frac{\zeta_1}{\sqrt{2\Gamma_0\Gamma_2}} \tag{41}$$

$$z_2 = \frac{\zeta_2}{\sqrt{2\Gamma_0\Gamma_1}} \tag{42}$$

The triad interaction equations then become

$$\dot{\zeta_0} = -i\zeta_1\zeta_2 \tag{43}$$

$$\dot{\zeta_1} = -\frac{i}{2}\zeta_0\zeta_2^* \tag{44}$$

$$\dot{\zeta_2} = -\frac{i}{2}\zeta_0\zeta_1^*, \tag{45}$$

plus the three complex conjugate equations.

Triad Interation Frequencies – Numerical Solution
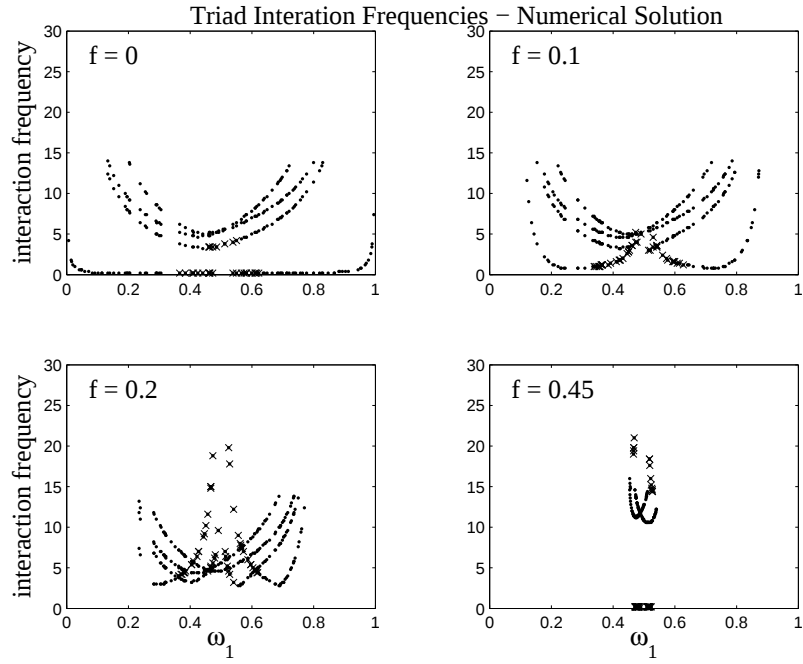
Figure 5: Interaction frequency for all possible resonant triads over a range of values of $\omega_{1,2}$, with everything else held constant. Points marked with an x denote triads where the vertical wavenumer of wave 1 is greater than five times that of wave 0.

Interaction Frequency as a Function of Γ_i
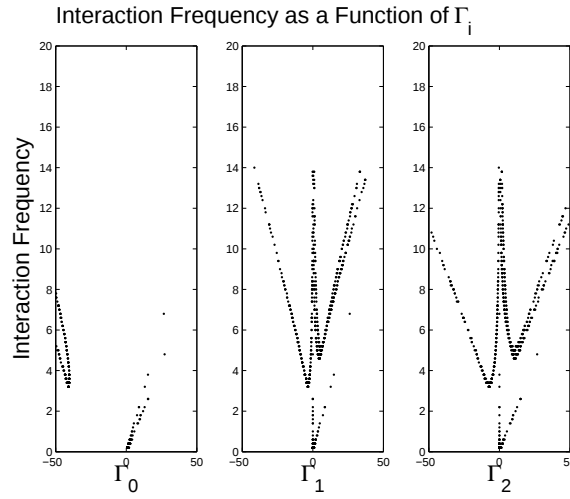
Figure 6: Interaction frequencies as a function of the three interaction coefficients, computed for a range of resonant triads with $f = 0$ and $\omega_0 = 1$.

174

Two invariants to the system are easily found. One is the energy,

$$|\zeta_0|^2 + |\zeta_1|^2 + |\zeta_2|^2 = A_0, \tag{46}$$

and another is given by one of the Manley-Rowe relations:

$$|\zeta_1|^2 - |\zeta_2|^2 = A_1. \tag{47}$$

Taking the time derivative of (43), and substituting (43) - (45) and their complex conjugates, and (46), gives

$$\ddot{\zeta}_0 = -i\frac{d(\zeta_1\zeta_2)}{dt} = -\frac{1}{2}\zeta_0\left(A_0 - |\zeta_0|^2\right). \tag{48}$$

This equation can be integrated twice to find an equation for $\zeta_0(t)$. (48) can be separated into its complex and imaginary components. Letting

$$\zeta_0 = u_0 e^{i\phi}, \tag{49}$$

(48) becomes

$$\ddot{u}_0 + i\dot{u}_o\dot{\phi}_0 + i\ddot{\phi}_0 u_0 + i\dot{\phi}_0\dot{u}_0 - \dot{\phi}_0{}^2 u_0 = -\frac{1}{2}u_0\left(A_0 - u_0^2\right). \tag{50}$$

The imaginary component of (50) is easily integrated:

$$
\begin{aligned}
\frac{\ddot{\phi}_0}{\dot{\phi}_0} + 2\frac{\dot{u}_0}{u_0} &= 0 \\
\rightarrow \ln\dot{\phi}_0 + \ln u_0^2 &= A_2 \\
\rightarrow \dot{\phi}_0 u_0^2 &= A_3
\end{aligned}
\tag{51}
$$

The real component of (50) can now be rewritten using (51):

$$\ddot{u}_0 - \frac{A_3}{u_0^3} = -\frac{1}{2}\left(A_0 u_0 - u_0^3\right). \tag{52}$$

This can be integrated as well, to give

$$\dot{u}_0{}^2 + \frac{A_3^2}{u_0^2} = -\frac{A_0}{2}u_0^2 + \frac{1}{4}u_0^4 + A_4. \tag{53}$$

Now writing $x = u_0^2$, we have

$$
\begin{aligned}
\dot{x}^2 &= x^3 - 2A_0 x^2 + 4A_4 x - 4A_3^2 \\
&=: -2\pi(x).
\end{aligned}
\tag{54}
$$

Now (54) can be written as an integrable ODE, of the form

$$\frac{1}{2}\left(dx/dt\right)^2 + \pi(x) = 0,$$

175
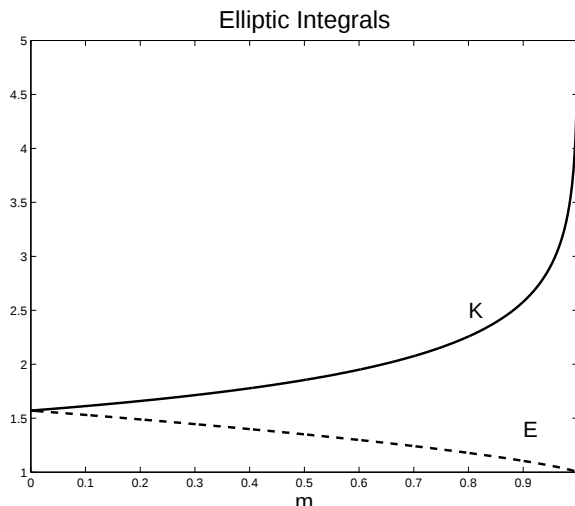
Figure 7: The complete elliptic integrals K and E as a function of the parameter m.

where $\pi(x)$ is a cubic function, with roots $a > b > c$.

If $\pi(x)$ has three real roots and $b < x(0) < a$, solutions $x(t)$ oscillate in a "potential well" bounded by the roots a and b. These oscillatory solutions are proportional to Jacobi Elliptic functions, with a period of

$$T = 2\sqrt{\frac{6}{a-c}}\left(cK(m) + (a-c)E(m)\right), \tag{55}$$

where K and E are the complete elliptic integrals of the first and second kind, respectively, and

$$m = \frac{a-b}{a-c}. \tag{56}$$

These are plotted in figure 7.

While this expression for the period is somewhat complicated, it can be interpreted in terms of the roots of $\pi(x)$, or the shape of the potential well. Assuming, for example, that the third root, c, stays constant, and letting $c = 0$, if the distance between the two largest roots increases (that is, if the size of the potential well increases), the parameter m will increase as well, E will go to zero, and T will decrease. If the distance between the largest and smallest root $(a - c)$ increases relative to $a - b$, then $m \to 0$, which means $K, E \to \pi/2$, and, again, T will decrease. The interaction frequency, therefore, can be interpreted in terms of the shape of $\pi(x)$.

The roots of $\pi(x)$ depend on the invariants in (54), which in turn depend on the initial wave amplitudes, as well as the interaction coefficients, which of course also depend on f. Figure 8 shows $\pi(x)$ plottted for $\omega_1 = .4$, and two values of f. As f approaches ω_1, the shape of $\pi(x)$ changes for one of the four solutions– the distance between the largest and smallest root becomes bigger, corresponding to a smaller interaction period (and higher interaction frequency).

Figure 9 shows the interaction frequency, computed analytically, for a range of ω_1, at four different values of f approaching the critical latitude, as in Figure 5.

176
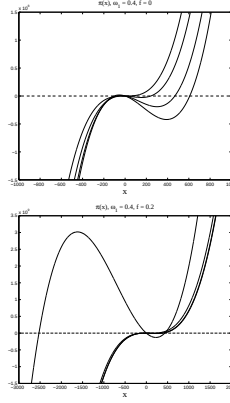
Figure 8: The potential function given in (54), for all 4 sets of resonant triads with $\omega_0 = 1$, and $\omega_1 = 0.2$. $f = 0$ in the top panel, and $f = 0.2$ in the bottom panel.
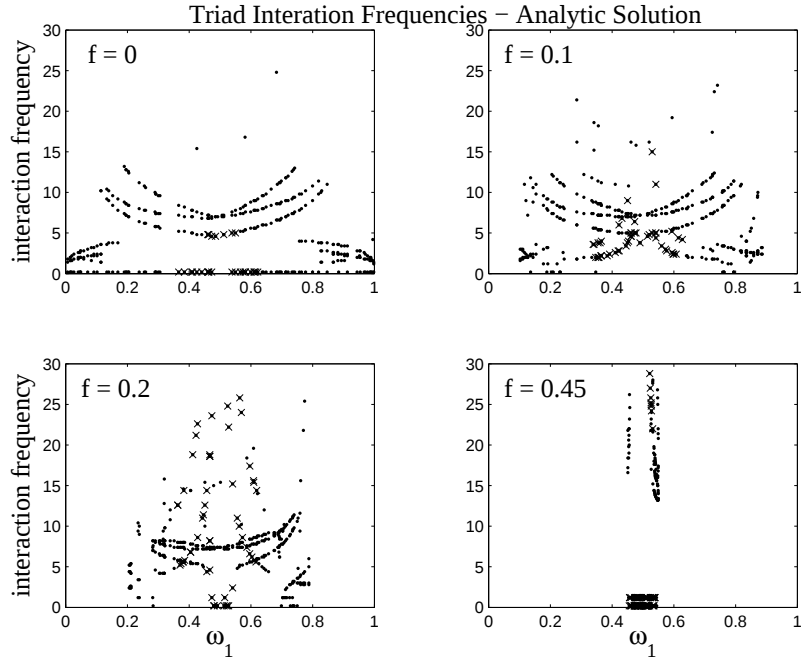

Figure 9: As in Fig. 5, but for the analytical solution given by (??): Interaction frequency for all possible resonant triads over a range of values of $\omega_{1,2}$, with everything else held constant. Points marked with an x denote triads where the vertical wavenumer of wave 1 is greater than five times that of wave 0.

As in the numerical integration of the triad equations and the above analytical reasonin, the interaction frequency at the subharmonic peak increases as f increases – thus showing that the behavior found in section 4 was not simply a numerical peculiarity.

5   Conclusions

This study has investigated the rate of energy transfer via triad resonance out of the internal M_2 tide .

- We have shown numerically that the efficiency of PSI increases as the waves approach the critical latitude where the Coriolis parameter f equals half the primary frequency, ω_0.

- This property is not simply a consequence of the fact that $\omega_0/2$ waves have zero group velocity at the critical latitude, but seems to be an intrinsic property of the triad equations.

- Since the triad equations are integrable, and analytical solution can be found, and the relationship between the system parameters, particularly f, and the interaction frequency can be examined more closely.

This study is a simple exercise intended to cast the more or less established and known properties of PSI into the context of the internal tide. Several things remain to be examined. A closer examination of the analytical solution and its relationship to f may be possible, especially if it is possible to cast the potential function $\pi(x)$ and its roots in a more transparent form. The problem should also be extended to the three dimensional ($l_i \neq 0$) case. The realistic numbers corresponding to the nondimensional results shown above (that is, an estimate of ϵ) also need to be considered.

6   Acknowldegements

7 Appendix

To derive the triad equations (37)-(39), we substitute (36) into (26), and apply the resonance condition,

$$\theta_0 = \theta_1 + \theta_2. \tag{57}$$

The modulation of wave 0 by the other two waves can be found by plugging

$$z_0(\tau)e^{i\theta_0(t)}, \tag{58}$$

where $z_0(\tau)$ is the slowly-varying, complex amplitude of wave 0, into the left hand side of (26), and expanding each term on the right hand side in terms of waves 1 and 2. The left hand side then becomes

$$2\frac{\partial^2}{\partial t \partial \tau}(\nabla^2 + \partial_{zz})z_0 e^{i\theta_0} = 2i\omega_0\left(k_0^2 + l_0^2 + m_0^2\right)\frac{\partial z_0}{\partial \tau}e^{i\theta_0}. \tag{59}$$

On the right hand side of (26), the first gradient term becomes

$$
\begin{aligned}
-\nabla^2(\mathbf{u}\cdot\nabla b) &= -\nabla^2\left(u_1\frac{\partial b_2}{\partial x} + v_1\frac{\partial b_2}{\partial y} + w_1\frac{\partial b_2}{\partial z} + u_2\frac{\partial b_1}{\partial x} + v_2\frac{\partial b_1}{\partial y} + w_2\frac{\partial b_1}{\partial z}\right) \\
&= -\nabla^2 i\left[(u_1 k_2 + v_1 l_2 + w_1 m_2)b_2 + (u_2 k_1 + v_2 l_1 + w_2 m_1)b_1\right].
\end{aligned}
$$

Substituting the polarizations relation between u and w, (22), and between b and w, (25), the right hand side becomes

$$-i\nabla^2 A_0 w_1 w_2,$$

where

$$
\begin{aligned}
A_0 w_1 w_2 &= [k_2 g_u(w_1) + l_2 g_v(w_1) + m_2 g_w(w_1)]g_b(w_2) \\
&+ [k_1 g_u(w_2) + l_1 g_v(w_2) + m_1 g_w(w_2)]g_b(w_1)
\end{aligned} \tag{60}
$$

Expanding the complex amplitudes and applying (57), the right hand side becomes

$$
\begin{aligned}
-i\nabla^2 A_0 z_1 z_2 e^{i\theta_1}e^{\theta_2} &= -i\nabla^2 A_0 z_1 z_2 e^{i\theta_0} \\
&= i\left(k_0^2 + l_0^2\right)A_0 z_1 z_2 e^{i\theta_0}.
\end{aligned} \tag{61}
$$

The other terms on the right hand side of (26) can be expanded in a similar way:

$$
\begin{aligned}
-\partial_t\nabla^2(\mathbf{u}\cdot\nabla w) &= \left(k_0^2 + l_0^2\right)\omega_0 B_0 z_1 z_2 e^{i\theta_0} & (62) \\
\partial_{zxt}(\mathbf{u}\cdot\nabla u) &= -m_0 k_0 \omega_0 C_0 z_1 z_2 e^{i\theta_0} & (63) \\
\partial_{zyt}(\mathbf{u}\cdot\nabla v) &= -m_0 l_0 \omega_0 D_0 z_1 z_2 e^{i\theta_0} & (64) \\
-f\partial_{zy}(\mathbf{u}\cdot\nabla u) &= i f m_0 l_0 C_0 z_1 z_2 e^{i\theta_0} & (65) \\
f\partial_{zx}(\mathbf{u}\cdot\nabla v) &= -i f m_0 k_0 D_0 z_1 z_2 e^{i\theta_0}. & (66)
\end{aligned}
$$

Now setting the expanded left hand side (59) equal to the combined terms on the right hand side (61) - (66), and we can solve for the rate of change of the complex amplitude of wave 0:

$$
\begin{aligned}
\frac{\partial z_0}{\partial \tau} &= \frac{-i}{2\omega_0\kappa_0} \left[\kappa_{H,0}^2(iA_0 + \omega_0 B_0) - m_0\omega_0(k_0 C_0 + l_0 D) + ifm_0(l_0 C_0 - k_0 D_0)\right] z_1 z_2 \\
&=: -i\Gamma_0 z_1 z_2
\end{aligned}
\tag{67}
$$

where

$$
\begin{aligned}
\kappa_0^2 &= k_0^2 + l_0^2 + m_0^2 \\
\kappa_{H,0}^2 &= k_0^2 + l_0^2.
\end{aligned}
$$

Equations for the modulation of waves 1 and 2 can be computed in a similar way, with a similar set of parameters $[A_1, B_1, C_1, D_1]$ and $[A_2, B_2, C_2, D_2]$ comprising the interaction coefficients Γ_1 and Γ_2.

References

[1] K. Polzin, J. Toole, J. Ledwell, and R. Schmitt, "Spatial variability of turbulent mixing in the abyssal ocean," Science **276**, 93 (1997).

[2] L. S. Laurent and C. Garrett, "The role of internal tides in mixing the deep ocean," J. Phys. Ocean. **32**, 2882 (2002).

[3] J. MacKinnon and K. Winters, "Tidal mixing hotspots governed by rapid parametric subharmonic instability," J. Phys. Ocean. **too appear**, (2004).

[4] D. Olbers and N. Pomphrey, "Disqualifying two candidates for the energy balance of oceanic internal waves," J. Phys. Ocean. **11**, 1423 (1981).